Amphiphilic organosilane-directed synthesis of crystalline zeolite with tunable mesoporosity

MINKEE CHOI, HAE SUNG CHO, RAJENDRA SRIVASTAVA, CHITHRAVEL VENKATESAN, DAE-HEUNG CHOI AND RYONG RYOO*

National Creative Research Initiative Center for Functional Nanomaterials and Department of Chemistry, Korea Advanced Institute of Science and Technology, Daejeon 305-701, Korea
*e-mail: rryoo@kaist.ac.kr

Published online: 6 August 2006; doi:10.1038/nmat1705

Zeolites are a family of crystalline aluminosilicate materials widely used as shape-selective catalysts, ion exchange materials, and adsorbents for organic compounds[1,2]. In the present work, zeolites were synthesized by adding a rationally designed amphiphilic organosilane surfactant to conventional alkaline zeolite synthesis mixtures. The zeolite products were characterized by a complementary combination of X-ray diffraction (XRD), nitrogen sorption, scanning electron microscopy (SEM) and transmission electron microscopy (TEM). The analyses show that the present method is suitable as a direct synthesis route to highly mesoporous zeolites. The mesopore diameters could be uniformly tailored, similar to ordered mesoporous silica with amorphous frameworks[3]. The mesoporous zeolite exhibited a narrow, small-angle XRD peak, which is characteristic of the short-range correlation between mesopores, similar to disordered wormhole-like mesoporous materials[4,5]. The XRD patterns and electron micrographs of the samples taken during crystallization clearly showed the evolution of the mesoporous structure concomitantly to the crystallization of zeolite frameworks. The synthesis of the crystalline aluminosilicate materials with tunable mesoporosity and strong acidity has potentially important technological implications for catalytic reactions of large molecules, whereas conventional mesoporous materials lack hydrothermal stability and acidity.

The design of rational synthesis pathways for porous materials is significant due to their potential applications as advanced catalysts, adsorbents, optical guides and sensors. In modern science, extensive research efforts have been devoted to the synthesis of porous inorganic materials with different structural coherency over a wide range of length scale. In particular, there have been extensive synthesis works on mesoporous aluminosilicate materials such as MCM-41 (ref. 3) and SBA-15 (ref. 6), using surfactant as a structure-directing agent. The mesopore diameters of the mesoporous materials were quite uniform, and furthermore, were finely tunable (typically, over the diameter range of 2–15 nm). Mesoporous materials have attracted much attention as a new adsorbent, catalyst support, and synthesis template for other nanostructured materials[2]. Particularly in catalysis, the mesoporous structure was very promising for reactions involving large molecular species, due to the possibility of overcoming the diffusion limitation with crystalline microporous zeolites (0.3–1.5 nm in pore diameter). The MCM-41-type mesoporous materials, however, exhibited insufficient hydrothermal stability and acidity compared with crystalline zeolites[7–9]. Material scientists thereafter endeavoured to improve the framework crystallinity for practical applications. Despite tremendous efforts, the hydrothermal stability and framework acidity were still far from the properties of crystalline zeolites.

Various attempts to synthesize mesoporous aluminosilicate materials with improved framework crystallinity were reported. In a typical approach, molecular templates for zeolites (for example, tetrapropylammonium and alkali metal ions) were added to the synthesis composition for ordinary mesoporous aluminosilicates[10–12]. The synthesis approach was based on the idea that the molecular templates could direct zeolite crystallization in the mesopore walls, while mesoporous structures are concurrently formed according to the supramolecular templating mechanism of the surfactant micelles. However, it turned out that the two different templating systems worked in a competitive, rather than a cooperative, manner. The syntheses mostly resulted in the formation of amorphous mesoporous material, bulk zeolite without mesoporosity, or their physical mixtures. One exceptional case was the synthesis of a lamellar mesostructure with a crystalline framework[13,14], but the structure collapsed into a non-porous material on calcination. Multi-step synthesis strategies were proposed to solve the phase-separation problem of the zeolite and mesoporous phases. In these strategies, the synthesis composition for conventional zeolite was hydrothermally aged until the primary or secondary building units for zeolite structure were formed. The resultant gel mixture, which was believed to contain zeolite

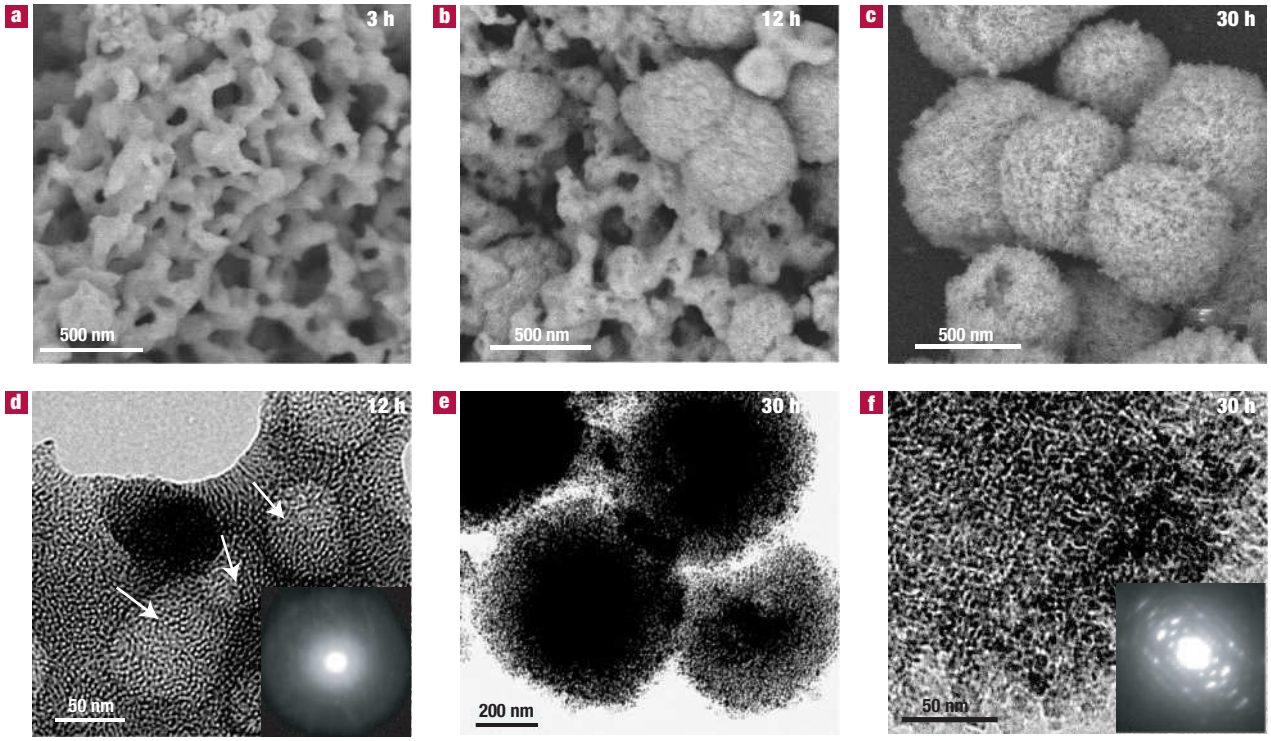

Figure 1 Electron microscopic investigation on the formation of mesoporous MFI zeolite. a–c, SEM and **d–f**, TEM images of the products precipitated after various reaction times during hydrothermal synthesis of mesoporous MFI zeolite at 150 °C. The SEM images show a distinct change in morphology, from a sponge-like macroporous network to globular particles with rugged surfaces. The TEM image in **d** shows that the initial phase was a mesoporous material with an amorphous framework. The TEM images in **e** and **f** and the corresponding electron diffraction pattern (inset of **f**) indicate that the final product was a mesoporous MFI zeolite with a polycrystalline framework. The initial phase gradually disappeared with the reaction time, leaving macrocavities (50–200 nm in diameter) within the remaining domain (arrows in **d**). This phenomenon indicates that the mesoporous zeolite particles were formed via the solution-mediated crystallization mechanism[1]. To observe the genuine surface structure, the SEM images were taken at a low electron acceleration voltage (2 kV, Hitachi S-4800), without metal coating[32]. TEM images were obtained using a Philips F20 Tecnai transmission electron microscope with an operating voltage of 200 kV. The TEM images were taken after mounting the zeolite particle on a porous carbon grid.

'seed' crystals, was assembled to mesoporous structure by the addition of surfactants[15–18]. Alternatively, the aged gel mixture was coated on the pore walls of pre-synthesized mesoporous silica[19,20]. The seed-assembled products exhibited well-defined small-angle X-ray diffraction (XRD) patterns, which were characteristic of an ordered mesoporous material. The seed-assembled products were claimed to be 'pseudozeolite' or 'protozeolite' in the framework nature, but these materials did not exhibit the long-range atomic order characteristic of a crystalline zeolite framework. Although the acidity and hydrothermal stability were somewhat improved, the properties were still far from those of crystalline zeolites[21], being insufficient for many industrial applications. Recently, it was also reported that mesoporous materials with crystalline zeolite framework can be synthesized through a crystallization process inside a packed bed of removable 'solid' nanotemplates (for example, carbon nanoparticles[22,23], nanotubes[24], mesoporous carbons[25], and polymer beads[26,27]). However, such a process using a solid template has limited pore tunability depending on the availability of templates.

Herein, we report a direct synthesis route to mesoporous zeolites with tunable mesoporous structure using the amphiphilic organosilanes as a mesopore-directing agent. As mentioned above, crystalline zeolite containing both micro- and mesoporous structures in a single phase is difficult to obtain if the aluminosilicate gel is directly crystallized in the presence of ordinary organic surfactants and molecular templates for zeolites. The phase-separation phenomenon indicates that the surfactants are expelled from the aluminosilicate domain during the zeolite crystallization process, making it difficult for the surfactants to modulate the zeolite crystal growth into a mesoporous structure. As revealed by biomineralization processes[28] and some successful synthesis works[29], organic molecules that are capable of a strong interaction with the growing crystal surface can effectively modulate the crystallization process of inorganic materials. In these respects, we used a rationally designed surfactant molecule with functional groups to enhance the interaction with growing zeolite crystals. The key for the design was to find amphiphilic surfactant molecules that contained a hydrolysable methoxysilyl moiety, a zeolite structure-directing group such as quaternary ammonium, and a hydrophobic alkyl chain moiety. It was expected that such amphiphilic organosilanes could strongly interact with growing crystal domains through the formation of covalent bonds with other SiO_2 and Al_2O_3 sources using the methoxysilyl moiety. To meet the requirements, we have synthesized [3-(trimethoxysilyl)propyl]hexadecyldimethylammonium chloride ($[(CH_3O)_3SiC_3H_6N(CH_3)_2C_{16}H_{33}]Cl$, TPHAC) and their structural analogues. These molecules contain a surfactant-like long-chain alkylammonium moiety and a hydrolysable methoxysilyl group, linked together by a Si–C bond, which is chemically stable under various zeolite synthesis conditions[30]. In a typical synthesis, a pre-calculated amount of TPHAC (4 mol% of the total silica source) was added to the initial synthesis

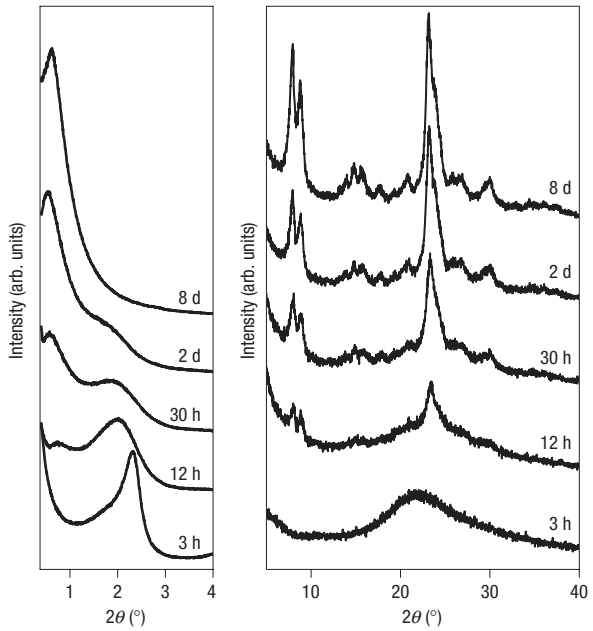

Figure 2 Powder XRD patterns for the products precipitated after various reaction times, during hydrothermal synthesis of mesoporous MFI zeolite at 150 °C. Small-angle XRD patterns were recorded in the reflection mode ($\lambda = 0.154250$ nm), using a synchrotron X-ray source of BL8C2 at Pohang Light Source. Wide-angle XRD patterns were taken with a Rigaku Multiflex diffractometer equipped with Cu Kα radiation (40 kV, 40 mA).

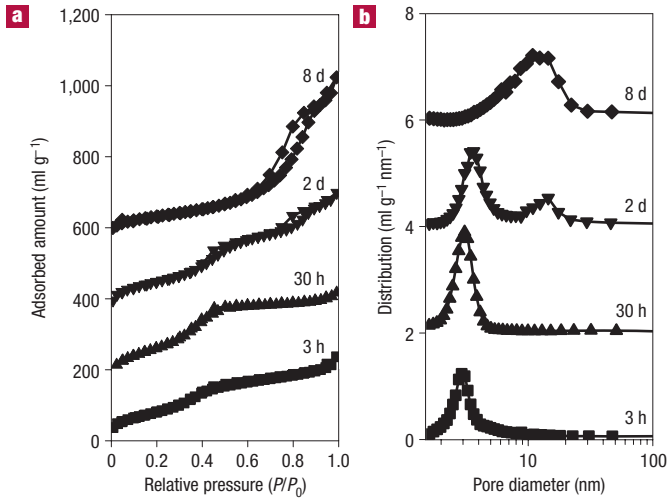

Figure 3 Pore structure analysis of the products precipitated after various reaction times during hydrothermal synthesis of mesoporous MFI zeolite at 150 °C. a, N_2 adsorption isotherms, and **b**, distribution of mesopore diameters. N_2 adsorption isotherms were measured at 77 K with a Quantachrome AS-1MP volumetric adsorption analyser. The isotherms for samples at 30 h, 2 d and 8 d were vertically offset by 100, 300 and 500 ml g^{-1}, respectively. Distributions of mesopore diameters were calculated via the Barrett–Joyner–Halenda (BJH) algorithm using the adsorption branch[33]. The distribution of mesoporous diameters for samples at 30 h, 2 d and 8 d were offset vertically by 2, 4 and 6 ml g^{-1} nm^{-1}, respectively.

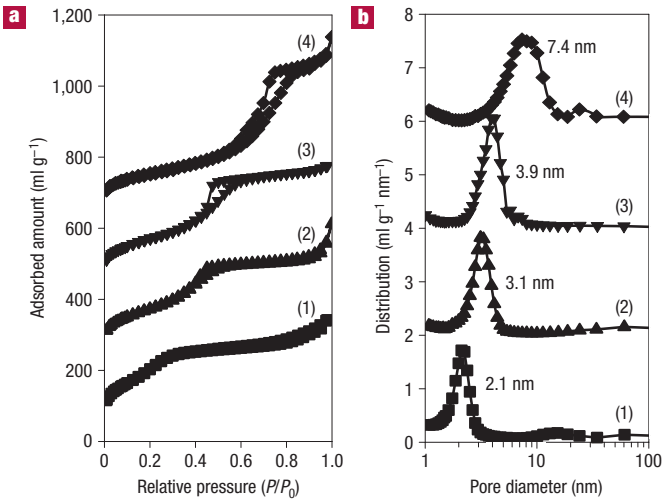

Figure 4 Mesoporous MFI zeolites with tunable mesopore diameters. a, N_2 adsorption isotherms for mesoporous MFI zeolites, and **b**, the corresponding pore size distribution (BJH). The isotherms for samples 2, 3 and 4 were vertically offset by 200, 400, 600 ml g^{-1}, respectively. The distribution of mesoporous diameters for samples 2, 3 and 4 were offset vertically by 2, 4 and 6 ml g^{-1} nm^{-1}, respectively. Samples 1–3 were synthesized by the hydrothermal reaction for 5 d at 130 °C, using organosilanes with different chain lengths ($[(CH_3O)_3SiC_3H_6N(CH_3)_2C_nH_{2n+1}]Cl$, $n = 12$, 16 and 18 for samples 1, 2 and 3, respectively). Sample 4 was synthesized for 2 d at 170 °C with $n = 16$.

composition of ordinary MFI zeolite (commonly known as ZSM-5), which included tetrapropylammonium ions (TPA^+) as a structure director for the zeolite. A conventional hydrothermal reaction was used for the crystallization. To systematically investigate the zeolite crystallization process, sample aliquots were periodically taken from a synthesis mixture for MFI zeolite (Si/Al = 14) during the hydrothermal reaction (see the Methods section), and were analysed by mutually complementary techniques such as transmission electron microscopy (TEM), scanning electron microscopy (SEM), XRD, ^{13}C cross-polarization magic-angle-spinning nuclear magnetic resonance (CP MAS NMR), and N_2 adsorption isotherm.

SEM and TEM (Fig. 1) revealed that a mesoporous aluminosilicate phase formed during the initial reaction period (<3 h), under the hydrothermal synthesis condition at 150 °C. The initial phase had a wormhole-type mesoporous structure with an amorphous framework, similar to previously reported mesoporous silicas[4,5]. ^{13}C CP MAS NMR analysis indicated that no significant amount of TPA^+ was included in the mesoporous phase. The formation of the mesoporous structure, exhibiting an XRD peak at $2\theta = 2.3°$ (Fig. 2), can be attributed to the supramolecular templating action of the amphiphilic organosilanes. As the reaction time proceeded (12 h), globular MFI zeolite particles began to form. The zeolite particle also had a highly mesoporous structure, as indicated by high-resolution SEM and TEM images. Moreover, the formation of the mesoporous zeolite particles was well supported by a small-angle XRD peak appearing at 0.7° and the wide-angle XRD peaks corresponding to the MFI zeolite structure. The electron microscopic investigation revealed that the amorphous domains gradually disappeared during this period. Macrocavities, about the size of 50–200 nm, were generated within the amorphous domain as a result of the phase loss by dissolution. Consequently, the XRD peak at 2.3° of the amorphous phases decreased in intensity. These changes support that the initial mesophase is dissolved into the solution, and then the mesoporous/microporous

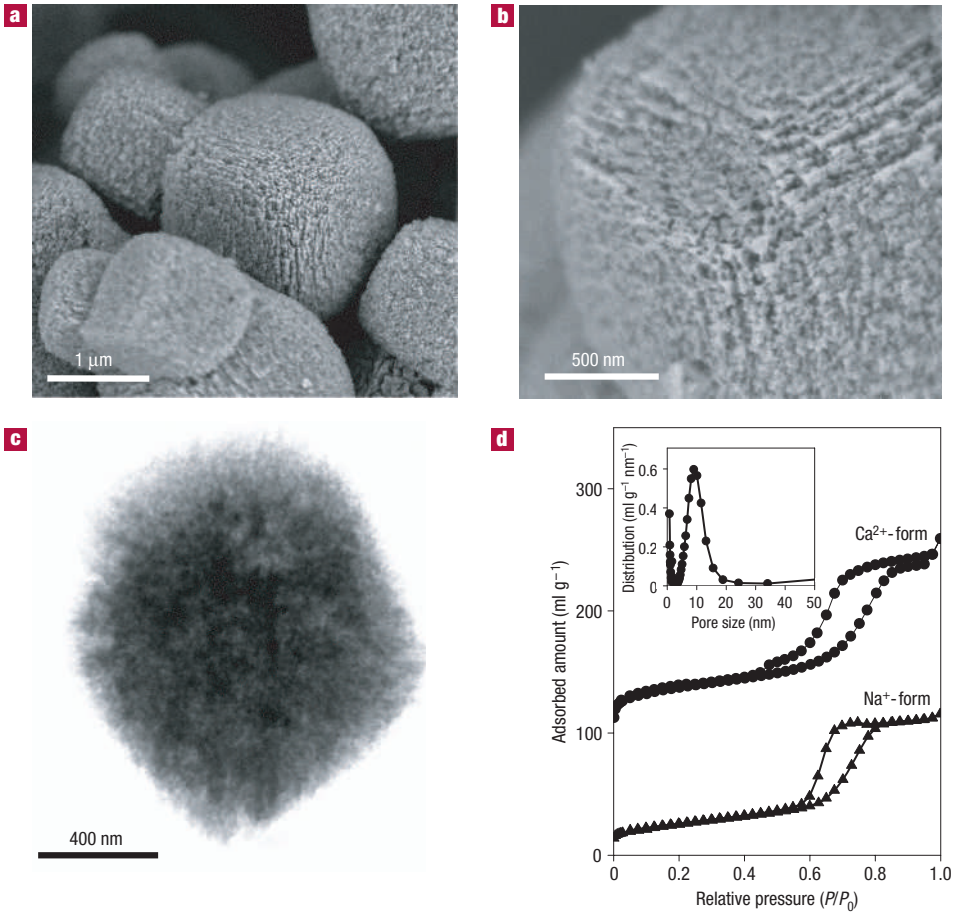

Figure 5 Mesoporous LTA zeolite synthesized using $[(CH_3O)_3SiC_3H_6N(CH_3)_2C_{16}H_{33}]Cl$. a,**b**, SEM images, **c**, TEM image, and **d**, pore size distribution from N_2 adsorption isotherm. Inset: Mesopore diameter distribution of Na^+ form.

zeolite crystals grow by using the dissolved species as the crystal nutrients. Such a solution-mediated crystallization mechanism is very common for zeolite synthesis under alkaline conditions[1]. A highly crystalline zeolite product was obtained after 30 h of reaction at 150 °C. Circular streaking in the electron diffraction pattern (Fig. 1) and the line broadening in the XRD peaks (Fig. 2) indicate that the mesoporous zeolite particles were built with randomly oriented zeolite nanocrystals. The zeolite (calcined at 550 °C) showed a type-IV isotherm with a narrow distribution of mesopore diameters centred at 3.1 nm (Fig. 3). On further heating to 8 d, however, the mesopore diameters increased to 8 nm. The globular morphology of the zeolite particles remained unchanged during the prolonged heating period, but a close examination of the SEM and TEM images revealed that the size of the nanocrystalline zeolites increased due to a ripening process (see Supplementary Information, Fig. S1). The change occurred more conspicuously at the external surface than at the core of the mesoporous zeolite particles, which could be because of faster molecular transport at the external surface. Such a crystal ripening process seemed to be the main reason for the mesopore enlargement, and can be significantly suppressed by lowering the crystallization temperature. For example, a highly crystalline MFI product with 3.1 nm mesopores was obtained after reaction for 5 d at 130 °C. The mesopore diameters and the pore volume were retained up to 12 d at 130 °C (see Supplementary Information, Fig. S2).

It is particularly noteworthy that the mesopore diameters of the MFI zeolite could be systematically varied, by changing the chain length of the organosilanes and/or the hydrothermal synthesis temperature (Fig. 4). The resultant mesopore diameters were very uniform as in MCM-41[3] and SBA-15[6]. As confirmed by XRD and electron microscopic investigations, the uniform mesoporosity was evidently coming from the zeolite phase. The mesoporous zeolite phase exhibited globular morphologies with rugged surfaces, which could be easily distinguished from the irregular morphologies of the amorphous mesophase. Careful electron microscopic investigation over a large number of specimens was used to confirm that there was no significant inclusion of bulk (not mesoporous) zeolite crystals or amorphous mesophase (see Supplementary Information, Fig. S3). Thus, it can be reasonably concluded that, within the limitations of the characterization, the samples were uniformly mesoporous in nature, being composed of crystalline zeolite frameworks. The MFI zeolite with mesoporous/microporous hierarchical structure could be synthesized with various Si/Al ratios above 14. The ^{27}Al MAS NMR spectrum (see Supplementary Information, Fig. S4) showed a single peak around 57–65 p.p.m., in agreement with tetrahedral Al sites in crystalline zeolite. No peaks owing to the extra-framework Al (octahedral coordination, 0–10 p.p.m.) were detected. It is also noteworthy that the present synthesis principle could be successfully extended to the synthesis of mesoporous LTA zeolite (Fig. 5). The N_2 adsorption isotherms of

Table 1 Catalytic properties of mesoporous MFI zeolite and other aluminosilicate materials.

Reactions*	Mesoporous MFI zeolite	Bulk ZSM-5	Al-MCM-41	SAM
Methanol to olefin/gasoline	86 (68/26/6)†	90 (67/28/5)	≪1 —	≪1 —
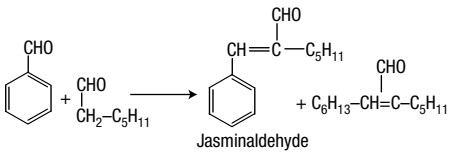 Jasminaldehyde	98 (98)‡	3.9 (69)	25 (79)	64 (75)
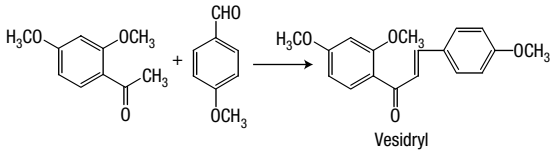 Vesidryl	60	3.3	10	35

* Catalytic activities were compared on the basis of the same weight of catalysts (see the Methods section for reaction conditions). All catalysts had the same Si/Al = 20. The Brunauer–Emmett–Teller (BET) surface area was 590 for mesoporous MFI, 350 for ZSM-5, 948 for AlMCM-41, and 923 $m^2\ g^{-1}$ for SAM (MCM-41-type).

† The numbers in parentheses represent % selectivity (olefin/gasoline/others).

‡ Jasminaldehyde selectivity. All other numbers indicate the reactant conversion (%).

the LTA zeolite exhibited two steep increases at relative pressures $(P/P_0) < 0.02$ and $0.7 < P/P_0 < 0.8$. These adsorptions were interpreted as micropore filling and capillary condensation in mesopores, respectively, similar to the case of mesoporous MFI zeolite.

The temperature-programmed desorption of ammonia was measured to characterize the acidity of the mesoporous MFI zeolite (H^+ form, Si/Al = 20). For comparison, bulk ZSM-5 zeolite, aluminosilicate MCM-41 (Al-MCM-41)[31], and ZSM-5 seed-assembled mesoporous (SAM) materials[16,18] were also synthesized and studied. The temperature-programmed desorption profiles (see Supplementary Information, Fig. S5) indicated that the mesoporous MFI zeolite possessed strong acid sites, similar to ZSM-5. In contrast, the Al-MCM-41 with amorphous framework showed only weak acid sites. The seed-assembled MCM-41 material showed a slightly enhanced acidity compared with Al-MCM-41[16], but was still much weaker than the mesoporous MFI zeolite and ZSM-5. Table 1 shows that the mesoporous MFI zeolite and ZSM-5 were similarly active (86 versus 90% conversion) in the transformation of methanol to olefin/gasoline. In contrast, the Al-MCM-41, seed-assembled MCM-41, and seed-assembled SBA-15[18] exhibited no measurable catalytic conversion. From these results, it is clear that the seed-assembled mesoporous materials possessing only a short-range atomic order ('pseudozeolitic' or 'protozeolite') cannot exhibit the true zeolite-like strong acidity. The results were also consistent with the nature of the reaction requiring strong acidity. The activity difference between the mesoporous MFI zeolite and ZSM-5 was not significant, owing to the small molecular size of the reactant and products.

The mesoporous structure with strong acidity can be a remarkable benefit for catalytic reactions involving large organic molecules, in which diffusion constraints and/or adsorption of reactant molecules onto the strong acid sites are the main concern. For example, the mesoporous MFI zeolite exhibited much higher catalytic activity and selectivity in the jasminaldehyde (α-*n*-amylcinnamaldehyde) synthesis reaction than bulk zeolite, Al-MCM-41 and MCM-41-type SAM (Table 1). The zeolite also exhibited an outstanding catalytic activity in the synthesis of vesidryl (2′,4,4′-trimethoxychalcone). These products are important for the pharmaceutical, fragrance, and agrochemical industries. The superior catalytic activity of the mesoporous zeolite compared with bulk zeolite is certainly due to the highly mesoporous structure. More notably, despite the significantly lower specific BET area, the mesoporous zeolite exhibited much higher catalytic activity than Al-MCM-41 and SAM materials. The crystalline zeolite with tunable mesoporosity may have important technological implications for many other catalytic reactions involving large molecules, whereas mesoporous materials with amorphous frameworks lack hydrothermal stability and acidity.

In conclusion, the mesoporous zeolite of the present study has several attractive features such as large surface area, interconnected mesopores with zeolitic pore walls, pore size control, facile synthesis on a large scale and so on. The mesopore diameters can be finely tuned, typically in the range of 2–20 nm, depending on the molecular structure of the mesopore-directing silanes and the hydrothermal synthesis conditions. The crystalline zeolites with tunable mesoporosity and strong acidity may bridge the gap between conventional bulk zeolite and amorphous mesoporous aluminosilicates, particularly for catalytic applications involving large molecules. Furthermore, the synthesis principle developed in the present work may be applied to other hierarchically structured materials. These materials with mesoporous/microporous hierarchical structures may find applications as advanced materials in various fields such as catalysis, adsorption, separation and sensor technologies.

METHODS

SYNTHESIS OF MESOPOROUS ZEOLITE

For the synthesis of mesoporous MFI zeolite, TPHAC was added to a conventional alkaline mixture containing TPABr, NaOH, tetraethylorthosilicate, sodium aluminate (53 wt% Al_2O_3, 43 wt% Na_2O, Riedel–deHaën) and distilled water. The molar composition of the mixture was 1 Al_2O_3/10 TPABr/10 Na_2O/38 SiO_2/1.6 TPHAC/7,200 H_2O. In a typical synthesis of MFI zeolite, 2.0 g sodium aluminate, 28.0 g TPABr and 8.0 g NaOH were first dissolved in 1,350 g H_2O. To the resultant solution, a mixture of 85.7 g tetraethylorthosilicate and 11.9 g TPHAC (66% methanol solution) was added under vigorous stirring. The final mixture was further stirred for 2 h at room temperature to obtain a homogeneous mixture. This mixture was heated with stirring at a desired temperature, in a Teflon-coated stainless-steel

autoclave. The precipitated product, after a certain reaction period, was filtered by suction, and washed with distilled water. The product was dried in an oven at 100 °C and subsequently calcined in air at 550 °C. Inductively coupled plasma analysis was used to determine the Si/Al ratio as 14. For the synthesis of mesoporous LTA zeolite, TPHAC was added to a mixture of sodium metasilicate ($Na_2SiO_3 \cdot 9H_2O$, Aldrich), NaOH, sodium aluminate and distilled water. The molar composition of the mixture was $1\ Al_2O_3/3.3\ Na_2O/2\ SiO_2/128\ H_2O/0.08$ TPHAC. After this mixture was heated with stirring in a polypropylene flask for 4 h at 95 °C, the crystallized zeolite product was filtered, washed with distilled water, dried at 110 °C and calcined at 550 °C. Other zeolites with various structures and mesoporosity can be synthesized using a variety of organosilanes (patent applied: 2005 Korean, and 2006 PCT).

CATALYTIC REACTIONS

A mesoporous MFI zeolite sample was prepared using TPHAC, under a slightly modified synthesis condition to give Si/Al = 20. For comparison, bulk ZSM-5 was synthesized from the same synthesis composition, but without TPHAC. Al-MCM-41[31] and SAM[16] materials with Si/Al = 20 were prepared following the reported procedures. All the synthesized materials were calcined and subsequently ion exchanged with NH_4^+ three times using 1 M NH_4NO_3 solution. These materials were calcined again at 550 °C to convert them into the H^+ form. For methanol-to-olefin/gasoline conversion, the catalyst samples were pressed, crushed and sieved to get particles of 14–20 mesh size. The catalytic reaction was carried out in a laboratory-built, down-flow stainless-steel reactor (10-mm inside diameter). Samples were analysed with an online gas chromatograph (equipped with a flame ionization detector, and a fused-silica capillary column). In a typical experiment, 100 mg of the sieved catalyst was diluted with five parts of 20-mesh sea sand. Before reaction, the catalyst was activated for 2 h at 550 °C in airflow. Methanol vapour was carried into the reactor by high-purity N_2 flow (WHSV = 7.9 h^{-1}, 65 ml min^{-1} flow rate) using a syringe pump. The reaction was carried out at 325 °C under atmospheric pressure.

For the catalytic syntheses of vesidryl and jasminaldehyde, reactions were carried out under N_2 atmosphere, using a Pyrex batch reactor equipped with a reflux condenser. In the vesidryl synthesis, 2,4-dimethoxy acetophenone (7 mmol), *p*-anisaldehyde (7 mmol) and catalyst (pre-activated at 150 °C, 50 mg powder) were mixed, and the reaction was conducted at 150 °C for 24 h. In the jasminaldehyde synthesis, heptanal (3 mmol), benzaldehyde (15 mmol) and catalyst (pre-activated at 150 °C, 50 mg) were mixed, and the reaction was conducted at 125 °C for 10 h. Samples after reaction were analysed by a gas chromatograph (equipped with a flame ionization detector and a packed column with 10% SE-30).

Received 3 February 2006; accepted 6 June 2006; published 6 August 2006.

References

1. Cundy, C. S. & Cox, P. A. The hydrothermal synthesis of zeolites: history and development from the earliest days to the present time. *Chem. Rev.* **103,** 663–701 (2003).
2. Corma, A. From microporous to mesoporous molecular sieve materials and their use in catalysis. *Chem. Rev.* **97,** 2373–2419 (1997).
3. Kresge, C. T. *et al.* Ordered mesoporous molecular-sieves synthesized by a liquid-crystal template mechanism. *Nature* **359,** 710–712 (1992).
4. Tanev, P. T. & Pinnavaia, T. J. A neutral templating route to mesoporous molecular sieves. *Science* **267,** 865–867 (1995).
5. Ryoo, R., Kim, J. M., Ko, C. H. & Shin, C. H. Disordered molecular sieve with branched mesoporous channel network. *J. Phys. Chem.* **100,** 17718–17721 (1996).
6. Zhao, D. Y. *et al.* Triblock copolymer syntheses of mesoporous silica with periodic 50 to 300 angstrom pores. *Science* **279,** 548–552 (1998).
7. Kim, J. M. & Ryoo, R. Disintegration of mesoporous structures of MCM-41 and MCM-48 in water. *Bull. Korean Chem. Soc.* **17,** 66–68 (1996).
8. Cassiers, K. *et al.* A detailed study of thermal, hydrothermal, and mechanical stabilities of a wide range of surfactant assembled mesoporous silicas. *Chem. Mater.* **14,** 2317–2324 (2002).
9. Zhao, D. *et al.* Comparison of disordered mesoporous aluminosilicates with highly ordered Al-MCM-41 on stability, acidity and catalytic activity. *Catal. Today* **68,** 11–20 (2001).
10. Beck, J. S. *et al.* Molecular or supramolecular templating: defining the role of surfactant chemistry in the formation of microporous and mesoporous molecular sieves. *Chem. Mater.* **6,** 1816–1821 (1994).
11. Karlsson, A., Stocker, M. & Schmidt, R. Composites of micro- and mesoporous materials: Simultaneous syntheses of MFI/MCM-41 like phases by a mixed template approach. *Micropor. Mesopor. Mater.* **27,** 181–192 (1999).
12. Petkov, N., Holzl, M., Metzger, T. H., Mintova, S. & Bein, T. Ordered micro/mesoporous composite prepared as thin films. *J. Phys. Chem. B* **109,** 4485–4491 (2005).
13. Christiansen, S. C. *et al.* Molecularly ordered inorganic frameworks in layered silicate surfactant mesophases. *J. Am. Chem. Soc.* **123,** 4519–4529 (2001).
14. Hedin, N. *et al.* Structure of a surfactant-templated silicate framework in the absence of 3D crystallinity. *J. Am. Chem. Soc.* **126,** 9425–9432 (2004).
15. Liu, Y., Zhang, W. Z. & Pinnavaia, T. J. Steam-stable aluminosilicate mesostructures assembled from zeolite type Y seeds. *J. Am. Chem. Soc.* **122,** 8791–8792 (2000).
16. Liu, Y., Zhang, W. Z. & Pinnavaia, T. J. Steam-stable MSU-S aluminosilicate mesostructures assembled from zeolite ZSM-5 and zeolite beta seeds. *Angew. Chem. Int. Edn* **40,** 1255–1258 (2001).
17. Zhang, Z. T. *et al.* Mesoporous aluminosilicates with ordered hexagonal structure, strong acidity, and extraordinary hydrothermal stability at high temperatures. *J. Am. Chem. Soc.* **123,** 5014–5021 (2001).
18. Liu, Y. & Pinnavaia, T. J. Assembly of hydrothermally stable aluminosilicate foams and large-pore hexagonal mesostructures from zeolite seeds under strongly acidic conditions. *Chem. Mater.* **14,** 3–5 (2002).
19. On, D. T. & Kaliaguine, S. Zeolite-coated mesostructured cellular silica foams. *J. Am. Chem. Soc.* **125,** 618–619 (2003).
20. Do, T. O. *et al.* Zeolite nanoclusters coated onto the mesopore walls of SBA-15. *J. Am. Chem. Soc.* **126,** 14324–14325 (2004).
21. Xia, Y. D. & Mokaya, R. Are mesoporous silicas and aluminosilicas assembled from zeolite seeds inherently hydrothermally stable? Comparative evaluation of MCM-48 materials assembled from zeolite seeds. *J. Mater. Chem.* **14,** 3427–3435 (2004).
22. Jacobsen, C. J. H. *et al.* Mesoporous zeolite single crystals. *J. Am. Chem. Soc.* **122,** 7116–7117 (2000).
23. Tao, Y. S., Kanoh, H. & Kaneko, K. ZSM-5 monolith of uniform mesoporous channels. *J. Am. Chem. Soc.* **125,** 6044–6045 (2003).
24. Schmidt, I. *et al.* Carbon nanotube templated growth of mesoporous zeolite single crystals. *Chem. Mater.* **13,** 4416–4418 (2001).
25. Sakthivel, A. *et al.* Replication of mesoporous aluminosilicate molecular sieves (RMMs) with zeolite framework from mesoporous carbons (CMKs). *Chem. Mater.* **16,** 3168–3175 (2004).
26. Holland, B. T., Abrams, L. & Stein, A. Dual templaing of macroporous silicates with zeolitic microporous frameworks. *J. Am. Chem. Soc.* **121,** 4308–4309 (1999).
27. Yang, X. Y. *et al.* Design and size control of uniform zeolite nanocrystals synthesized in adjustable confined voids formed by recyclable monodisperse polymer spheres. *Angew. Chem. Int. Edn* **44,** 2563–2568 (2005).
28. Kröger, N., Deutzmann, R. & Sumper, M. Polycationic peptides from diatom biosilica that direct silica nanosphere formation. *Science* **286,** 1129–1132 (1999).
29. Qiu, S. R. *et al.* Modulation of calcium oxalate monohydrate crystallization by citrate through selective binding to atomic steps. *J. Am. Chem. Soc.* **127,** 9036–9044 (2005).
30. Hűttinger, K. J. & Jung, M. F. Kinetik der synthese von trialkyl[-3-(trimethoxysilyl)-propyl]-ammoniumchloriden und deren antimikrobielle wirkung als fixierte biozide. *Chem. Ing. Tech.* **61,** 258–259 (1989).
31. Jun, S. & Ryoo, R. Aluminum impregnation into mesoporous silica molecular sieves for catalytic application to Friedel–Crafts alkylation. *J. Catal.* **195,** 237–243 (2000).
32. Che, S. *et al.* Direct observation of 3D mesoporous structure by scanning electron microscopy (SEM): SBA-15 silica and CMK-5 carbon. *Angew. Chem. Int. Edn* **42,** 2182–2185 (2003).
33. Barrett, E. P., Joyner, L. G. & Halenda, P. P. The determination of pore volume and area distributions in porous substances. I. Computations from nitrogen isotherms. *J. Am. Chem. Soc.* **73,** 373–380 (1951).

Acknowledgements

This work was supported by the Ministry of Science and Technology through the Creative Research Initiative Program, and by the School of Molecular Science through the Brain Korea 21Project. Synchrotron radiation XRD was supported by Pohang Light Source. The authors are grateful to S. Bai, and I. Lee for helpful discussions on electron microscopy.
Correspondence and requests for materials should be addressed to R.R.
Supplementary Information accompanies this paper on www.nature.com/naturematerials.

Competing financial interests

The authors declare that they have no competing financial interests.